

# Early Prediction of Liver Cirrhosis Up to Three Years in Advance: A Machine Learning Study Benchmarking Against the FIB-4 Score

Zhuqi Miao<sup>a,b</sup>, Sujan Ravi<sup>c</sup>, Abdulaziz Ahmed<sup>d,\*</sup>

<sup>a</sup>Center for Health Systems Innovation, Oklahoma State University, Tulsa, OK, 74119, USA

<sup>b</sup>Department of Management Science and Information Systems, Oklahoma State University, Stillwater, OK, 74106, USA

<sup>c</sup>Division of Gastroenterology and Hepatology, Department of Medicine, University of Alabama at Birmingham, Birmingham, AL, 35233, USA.

<sup>d</sup>Department of Health Services Administration, University of Alabama at Birmingham, Birmingham, AL, 35233, USA

\*Corresponding Author: Abdulaziz Ahmed, Email: [aahmed2@uab.edu](mailto:aahmed2@uab.edu)

## Abstract

**Objective:** Develop and evaluate machine learning (ML) models for predicting incident liver cirrhosis one, two, and three years prior to diagnosis using routinely collected electronic health record (EHR) data, and to benchmark their performance against the FIB-4 score.

**Methods:** We conducted a retrospective cohort study using de-identified EHR data from a large academic health system. Patients with fatty liver disease were identified and categorized into cirrhosis and non-cirrhosis cohorts based on ICD-9/10 codes. Prediction scenarios were constructed using observation and prediction windows to emulate real-world clinical use. Demographics, diagnoses, laboratory results, vital signs, and comorbidity indices were aggregated from the observation window. XGBoost models were trained for 1-, 2-, and 3-year prediction horizons and evaluated on held-out test sets. Model performance was compared with FIB-4 using area under the receiver operating characteristic curve (AUC).

**Results:** Final cohorts included 3,043 patients for the 1-year prediction, 1,981 for the 2-year prediction, and 1,470 for the 3-year prediction. Across all prediction windows, ML models consistently outperformed FIB-4. The XGBoost models achieved AUCs of 0.81, 0.73, and 0.69 for 1-, 2-, and 3-year predictions, respectively, compared with 0.71, 0.63, and 0.57 for FIB-4. Performance gains persisted with longer prediction horizons, indicating improved early risk discrimination.

**Conclusions:** Machine learning models leveraging routine EHR data substantially outperform the traditional FIB-4 score for early prediction of liver cirrhosis. These models enable earlier and more accurate risk stratification and can be integrated into clinical workflows as automated decision-support tools to support proactive cirrhosis prevention and management.

**Keywords:** liver cirrhosis, early disease prediction, machine learning, FIB-4 score.

## Introduction

Liver cirrhosis is the final stage of chronic liver disease and a leading cause of morbidity and mortality worldwide.<sup>1</sup> It develops silently over years, often without symptoms until the disease has progressed to an advanced stage.<sup>2,3</sup> Patients with liver cirrhosis are associated with reduced survival, increased hospitalization rates, and significant economic burden on health systems. In the United States, chronic liver disease and cirrhosis contribute a substantial share of the national health burden. Mortality from cirrhosis rose by nearly 90 percent over the past three decades, increasing from about 35,000 deaths in 1990 to more than 65,000 in 2019. Cirrhosis ranked as the 11th leading cause of death in 2019 and accounted for over 2 percent of all deaths.<sup>3</sup>

Early identification of patients at high risk is critical, because timely intervention can slow progression, guide treatment decisions, and prevent complications such as hepatic decompensation, hepatocellular carcinoma, and death.<sup>4,5</sup> Despite the importance of accurate staging, current tools for routine risk assessment have limitations. Liver biopsy remains the gold standard for diagnosing liver disease, characterizing masses, and grading inflammation, fibrosis, and steatosis. It provides detailed histology but carries procedural risks, requires specialized expertise, and is not suitable for repeated monitoring.<sup>6,7</sup> Newer approaches such as liquid biopsy and digital pathology are emerging and may reduce reliance on conventional biopsy, although their sensitivity and specificity remain suboptimal.<sup>8</sup> Over the past decades, non-invasive tests have become more widely used to assess liver disease. FibroScan (transient elastography) is considered the most reliable non-invasive method for evaluating liver fibrosis and is widely accepted, provides rapid results, and demonstrates high patient acceptability. However, it is limited by high costs and lack of availability in smaller cities, confining its routine use to tertiary care centers and specialty hospitals.<sup>9</sup>

To overcome these barriers, researchers and clinicians have developed simple serum-based indices such as the Fibrosis-4 (FIB-4) and Fibrofast (FIB-5) scores.<sup>10,11</sup> These formulas rely on laboratory and demographic variables that are readily available in routine care.<sup>10,11</sup> FIB-4 is calculated from age, platelet count, aspartate aminotransferase (AST), and alanine aminotransferase (ALT). FIB-5 is based on albumin, alkaline phosphatase, platelet count, and the AST to ALT ratio.<sup>10,11</sup> These indices are based on routinely available laboratory parameters, are inexpensive to calculate, and can be implemented in primary care without the need for specialized equipment. Evidence supports their usefulness as rule-out tools for advanced fibrosis. In a study of patients with non-alcoholic fatty liver disease, FIB-4 achieved an AUROC of 0.712 and FIB-5 achieved an AUROC of 0.655 for advanced fibrosis. Both scores demonstrated high negative predictive values, above 90 percent, which makes them helpful for excluding advanced disease in low-risk patients. At the same time, their diagnostic limitations are clear. For example, at the recommended cutoff of <2.02, FIB-4 had sensitivity of only 46.8 percent and specificity of 86.4 percent. At the <-7.11 cutoff, FIB-5 had higher sensitivity of 81.8 percent but lower specificity of 46.8 percent. These tradeoffs demonstrate the limited capacity of these scores to provide reliable risk stratification across diverse populations.

To address these limitations, several serum-based indices have been developed, including the Fibrosis-4 (FIB-4) and Fibrofast (FIB-5) scores.<sup>10,11</sup> Both rely on laboratory and demographic variables that are routinely available in clinical practice. FIB-4 is derived from age, platelet count, aspartate aminotransferase (AST), and alanine aminotransferase (ALT), whereas FIB-5 incorporates albumin, alkaline phosphatase, platelet count, and the AST to ALT ratio.<sup>10,11</sup> These

indices are inexpensive to calculate, require no specialized equipment, and can be applied in primary care settings. Evidence supports the use of these indices as rule-out tools for advanced fibrosis. In a cohort of patients with non-alcoholic fatty liver disease, Kumari et al.<sup>10</sup> reported that FIB-4 achieved an AUROC of 0.712 and FIB-5 achieved an AUROC of 0.655 for detecting advanced fibrosis. Both indices showed negative predictive values above 90 percent, meaning that patients classified as low risk were almost always free of advanced disease. At the same time, diagnostic accuracy was limited. At the  $<2.02$  cutoff, FIB-4 identified only 46.8 percent of patients with advanced fibrosis (sensitivity, true positives) while correctly classifying 86.4 percent of patients without advanced fibrosis (specificity, true negatives). This also means that more than half of patients with advanced disease were missed (false negatives). At the  $<7.11$  cutoff, FIB-5 identified 81.8 percent of patients with advanced fibrosis (sensitivity) but correctly excluded only 46.8 percent of those without advanced disease (specificity), leading to a high rate of false positives. These tradeoffs indicate that while both scores are useful for excluding advanced fibrosis, they are not sufficiently reliable for accurate risk stratification across diverse populations.

The limited diagnostic performance of FIB-4 and FIB-5 reflects their structural simplicity. Both indices apply fixed linear weights to a small set of laboratory parameters, without accounting for nonlinear associations or the wider set of demographics, biochemical, and clinical variables that contribute to disease progression. Fibrosis and cirrhosis arise from complex, multifactorial processes involving metabolic dysfunction, chronic inflammation, genetic predisposition, and comorbid conditions. Static formulas such as FIB-4 and FIB-5 are unable to adapt to these patterns. Consequently, while they are useful for screening and for ruling out advanced fibrosis in low-risk populations, they lack the precision required for clinical decision support in contexts where accurate staging is essential for treatment and referral.

Machine learning offers a potential solution to these limitations. Unlike traditional scores, ML algorithms are data-driven and capable of integrating a broader range of predictors. They can capture nonlinear relationships, model complex feature interactions, and improve in performance as larger datasets become available. In hepatology and related fields, ML approaches have been applied successfully to predict outcomes including hepatocellular carcinoma, portal hypertension, and mortality, with performance generally exceeding that of conventional regression-based risk scores. These findings suggest that ML is well suited to enhance the prediction of cirrhosis, particularly when benchmarked directly against indices such as FIB-4 and FIB-5.

## Methods

### Data Source and Extraction

This study utilized de-identified electronic health record (EHR) data from the University of Alabama at Birmingham (UAB) Informatics for Integrating Biology and the Bedside (i2b2) database to identify candidate patients. The UAB-i2b2 database contains structured hospital and outpatient clinical records derived from the enterprise EHR system and clinical data warehouse, encompassing encounters across the UAB healthcare system. All data were de-identified in compliance with the Health Insurance Portability and Accountability Act (HIPAA), and the study was exempted from Institutional Review Board (IRB) review at UAB.

In the extraction process, we first identified patients with fatty liver disease using ICD-9-CM code 571.8 and ICD-10-CM code K76.0. These patients were then categorized into two cohorts: liver cirrhosis (LC) and non-LC. LC was defined using ICD-9-CM codes 571.2 and 571.3 and ICD-10-CM codes K74.6x and K70.3x. For both cohorts, we extracted biomarkers that included six demographic variables, all diagnoses represented by ICD-9/10-CM codes, nine laboratory test results represented by LOINC codes, and three vital signs. A detailed list of all biomarkers is provided in Table 1.

Table 1: The diagnosis codes for patient extraction and the biomarkers for analysis.

Diagnosis Codes for Data Extraction	Diagnosis Code Description
Fatty Liver	
571.8	Other chronic nonalcoholic liver disease
K76.0	Fatty (change of) liver, not elsewhere classified
Liver Cirrhosis	
571.2	Alcoholic cirrhosis of liver
571.3	Alcoholic liver damage
K70.3x	Alcoholic cirrhosis of liver
K74.6x	Other and unspecified cirrhosis of liver
<b>Patient Biomarkers</b>	<b>Details/Descriptions</b>
Demographics	Date of birth (shifted for deidentification purpose), gender, race, marital status, county, state
Diagnoses	ICD-9-CM: 8,347 unique codes included ICD-10-CM: 27,441 unique codes included
Laboratory Test Results (LOINC)	
1742-6	Alanine aminotransferase (ALT)
1751-7	Albumin
1920-8	Aspartate aminotransferase (AST)
6768-6	Alkaline phosphatase (ALP)
1975-2	Bilirubin, total in serum or plasma
718-7	Hemoglobin
26515-7	Platelets
2885-2	Protein, total
5902-2	Prothrombin time (PT)
Vital Signs	Systolic blood pressure (SBP) Diastolic blood pressure (DBP) Body mass index (BMI)
Derived Variables	Age at prediction Charlson comorbidity index Rural-urban status

## Data Preparation

Once the data were extracted, although retrospective, we organized it to emulate a real-world prediction scenario.<sup>12,13</sup> Specifically, for each LC patient, we first identified the initial LC diagnosis, as illustrated in Figure 1. We then defined two time windows:

- Prediction Window: spans one, two, or three years prior to the diagnosis. Data within this window are excluded from modeling.
- Observation Window: immediately precedes the prediction window and extends as far back as available. Aggregated data within this window are used for prediction.

This approach allows us to leverage all historical data to predict the onset of LC within one, two, or three years. The three prediction window lengths were selected to align with the typical clinical timeline of periodical checkups for LC.

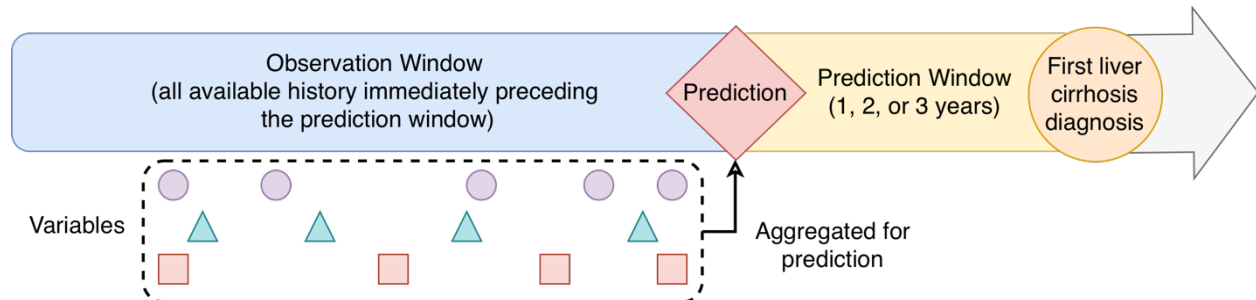


Figure 1. Illustration of data organization, with prediction and observation windows and data aggregation, used to emulate the prediction scenario.

With respect to aggregation, diagnoses were first grouped into higher-level, common-sense medical problems using the CCS system.<sup>14,15</sup> These CCS-based conditions were then transformed into binary variables based on whether the corresponding diagnosis codes occurred during the observation window: 1 if present, 0 otherwise. For demographic variables, values at the prediction point, i.e., one, two, or three years before the first LC diagnosis, were used. We also linked patients' locations to the 2023 Rural-Urban Continuum Codes (RUCC)<sup>16</sup> to determine their rural/urban status at the prediction point for analysis. For numerical variables, such as laboratory tests and vital signs, we used the average values across the observation window. Additionally, we derived the Charlson comorbidity index (CCI)<sup>17</sup> for each encounter and used the average CCI across the observation window for prediction.

To construct the non-LC cohort, we first selected patients who never had LC. In preliminary experiments, we observed that many non-LC patients had encounters much more recent than the prediction points of LC patients. Using these recent encounters as prediction points for the non-LC cohort resulted in observation windows containing diagnosis codes that were infrequent in the LC cohort, likely because these codes are relatively new and the LC cohort's observation windows were earlier. To address the issue, we identified encounters from non-LC patients that aligned with the prediction times of LC patients. Specifically, for each LC patient, we selected five non-LC patient encounters occurring within one week before or after that LC patient's prediction time. All selected non-LC encounters were then combined and filtered to retain only unique patients, as illustrated in Figure 2. This approach emulates a realistic recruitment scenario in which LC and non-LC patients are enrolled within the same one-week window for analysis.

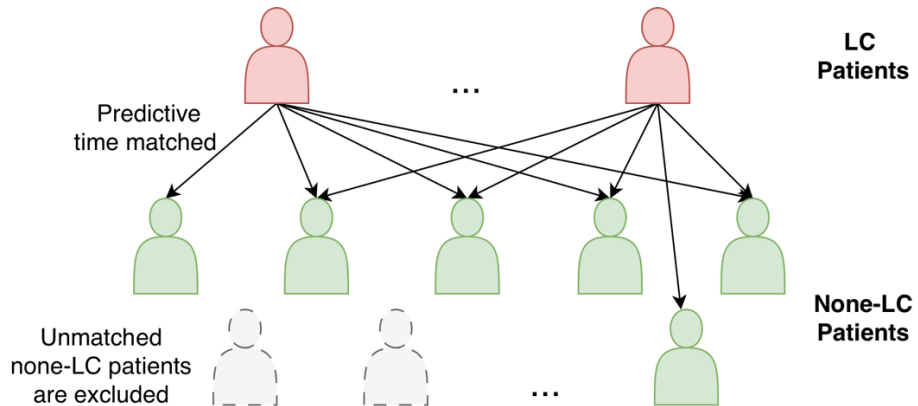


Figure 2. Illustration of the matching process. “Matched time” indicates that the encounters occurred no more than a week apart.

## Modeling

We developed three XGBoost<sup>18,19</sup> predictive models using three different prediction windows (one, two, and three years) and their corresponding cleaned datasets. For each model, the data was split into training and testing sets using a 70/30 ratio. The models were trained on the training dataset and evaluated on the testing dataset, as illustrated in Figure 3. The predictive performance of XGBoost was then compared with that of FIB-4<sup>10,20</sup> using the testing dataset.

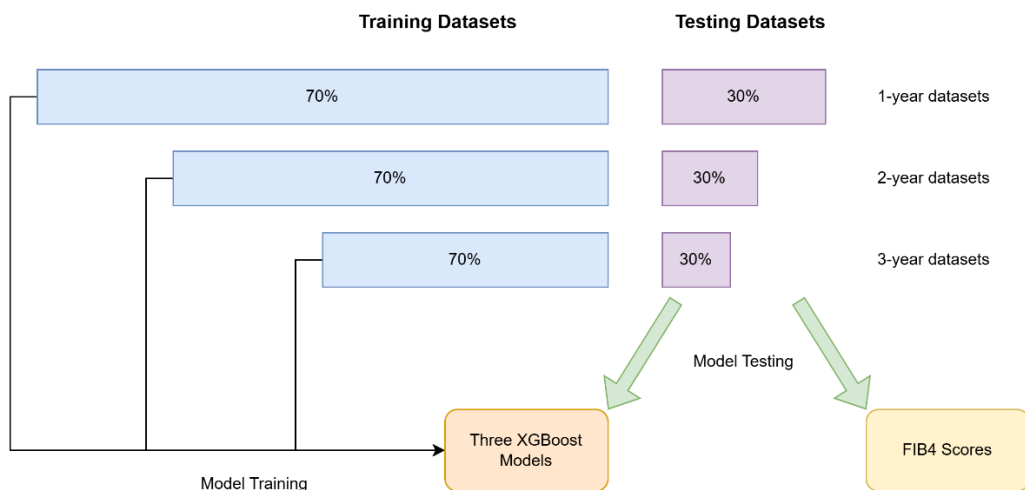


Figure 3. Schematic of the model training and testing process using multi-year datasets.

## Results

Figure 4 illustrates the cohort filtering process. We initially identified 30,550 patients with fatty liver disease from the data source, including 4,750 patients with LC and 25,800 without LC. After matching prediction dates, 10,551 non-LC patients remained. When restricting the analysis to complete-case data for different prediction windows, the final cohorts consisted of 904 cases (LC patients) and 2,139 controls (non-LC patients) for the 1-year prediction window; 508 cases and 1,473 controls for the 2-year prediction window; and 371 cases and 1,099 controls for the 3-year prediction window.

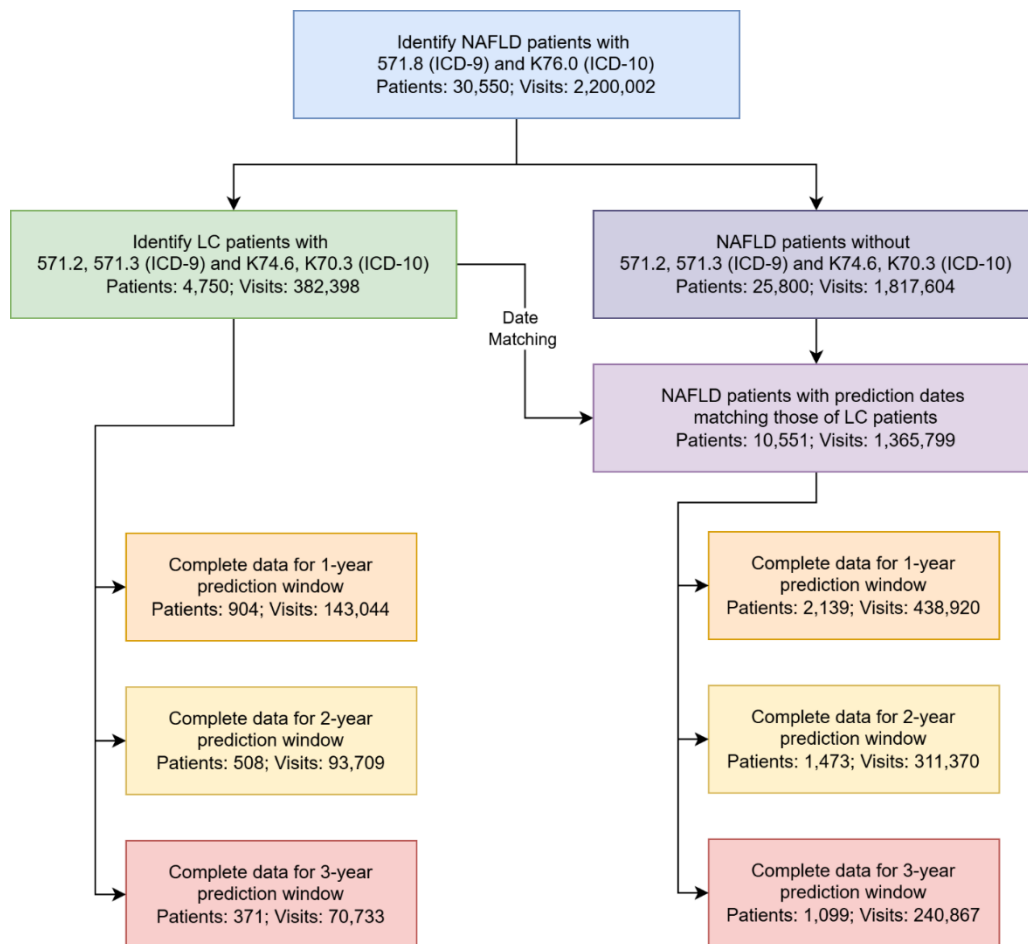


Figure 4. Flowchart showing the data extraction and cohort derivation process.

The cohort characteristics for the 1-year prediction are presented in Table 2, while those for the 2- and 3-year predictions are provided in Table A1 and Table A2 in the Appendix. Among demographic variables, gender and rural-urban status are significantly associated ( $p < 0.05$ ) with LC onset across the 1-, 2-, and 3-year prediction windows. Among vital signs, mainly BMI shows a significant association, and this is observed for the 2- and 3-year predictions. In addition, all evaluated laboratory measures, except hemoglobin and albumin, are strongly associated with LC risk across all prediction windows. Though insignificant for the 3-year prediction, albumin is significant for the 1- and 2-year predictions.

Diseases that are prevalent in the cohort and significantly associated with LC across all prediction windows include nutritional, endocrine, and metabolic disorders; liver diseases; lower respiratory diseases; gastrointestinal disorders; connective tissue diseases; nervous system disorders; spondylosis; back problems; and disorders of lipid metabolism, among others.

Table 2. Cohort characteristics for the 1-year prediction

	Overall	Controls	Cases	p-value
Patient Counts	3043	2139	904	
Gender				<0.001
Female	1767	1295	472	
Male	1275	843	432	
Unknown	1	1	0	
Race				<0.001
Native American	5	4	1	
Asian	83	63	20	
Black	973	748	225	
Decline	11	10	1	
Hispanic	29	23	6	
Multiple	1	1	0	
White	1941	1290	651	
Marital Status				0.715
Divorced	362	261	101	
Life Partner	14	12	2	
Married	1457	1024	433	
Separated	41	30	11	
Single	852	585	267	
Unknown	54	38	16	
Widowed	263	189	74	
Rural-Urban Status				<0.001
Metro, ≥1 million	2235	1683	552	
Metro, 250,000 to 1 million	221	115	106	
Metro, <250,000	198	107	91	
Nonmetro, ≥20,000, adjacent to metro	176	110	66	
Nonmetro, ≥20,000, not adjacent to metro	18	9	9	
Nonmetro, 5,000 to 20,000, adjacent to metro	61	36	25	
Nonmetro, 5,000 to 20,000, not adjacent to metro	12	7	5	
Nonmetro, <5,000, adjacent to metro	75	46	29	
Nonmetro, <5,000, not adjacent to metro	47	26	21	
Age, mean (SD)	55.8 (13.3)	55.5 (13.9)	56.8 (11.9)	0.008
Vitals/Labs, mean (SD)				
CCI	0.3 (0.4)	0.3 (0.4)	0.4 (0.4)	<0.001
BMI	33.1 (8.3)	33.5 (8.5)	32.3 (7.7)	<0.001
DBP	79.2 (7.2)	79.3 (7.1)	79.0 (7.4)	0.246
SBP	131.8 (12.7)	131.6 (12.5)	132.3 (13.3)	0.193
ALT (LOINC: 1742-6)	36.4 (36.6)	33.1 (36.6)	44.2 (35.6)	<0.001
Albumin (LOINC: 1751-7)	4.1 (4.6)	4.2 (5.5)	3.8 (0.5)	<0.001
AST (LOINC: 1920-8)	36.4 (32.7)	31.3 (29.3)	48.4 (36.8)	<0.001
Bilirubin (LOINC: 1975-2)	0.7 (0.7)	0.6 (0.5)	1.0 (0.8)	<0.001
Platelets (LOINC: 26515-7)	227.9 (89.3)	243.2 (81.4)	191.7 (96.5)	<0.001
Protein (LOINC: 2885-2)	7.0 (0.6)	7.0 (0.5)	7.1 (0.6)	0.005
PT (LOINC: 5902-2)	14.3 (2.7)	14.2 (2.6)	14.8 (3.0)	<0.001
ALP (LOINC: 6768-6)	92.4 (66.5)	85.0 (42.9)	109.9 (100.5)	<0.001
Hemoglobin (LOINC: 718-7)	12.9 (1.7)	12.9 (1.7)	13.0 (1.8)	0.562

The receiver operating characteristic (ROC) curves and corresponding areas under the ROC curves (AUCs) for the XGBoost models and FIB-4 are shown in Figure 5. Across all prediction windows, the machine-learning models consistently outperformed FIB-4, achieving at least a 10% higher AUC. Specifically, the AUCs for the XGBoost models versus FIB-4 were 0.81 vs 0.71 for the 1-year window, 0.73 vs 0.63 for the 2-year window, and 0.69 vs 0.57 for the 3-year window.

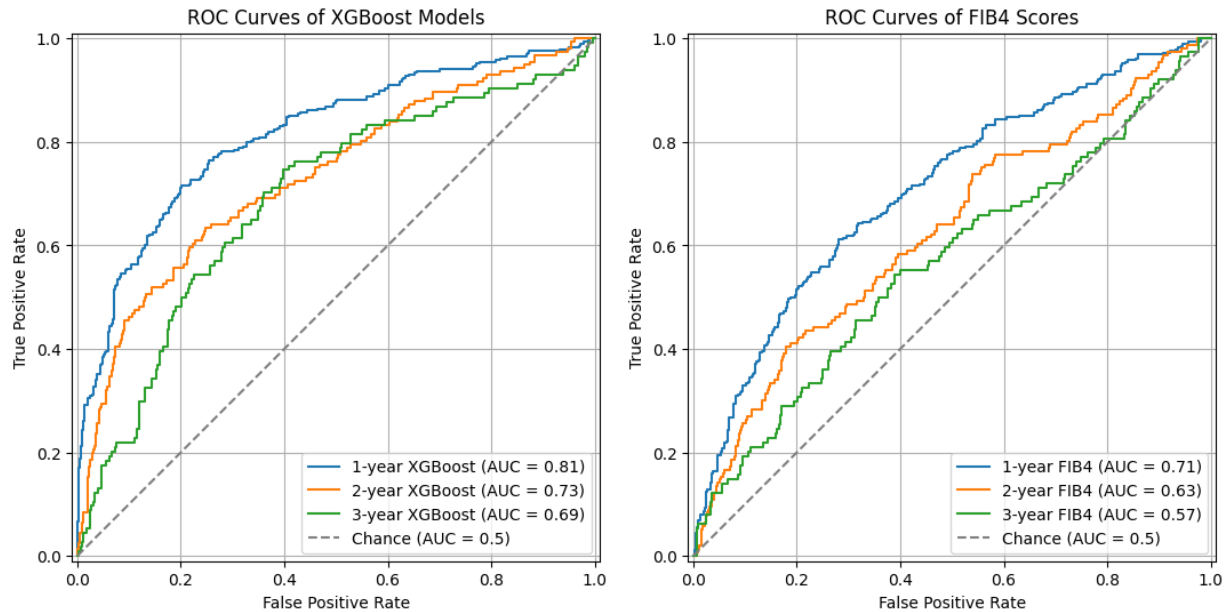


Figure 5. ROC curves for 1-, 2-, and 3-year predictions using XGBoost models vs. FIB-4 scores

## Discussion

In this study, we demonstrate that machine learning-based prediction models substantially outperform the commonly used FIB-4 score for identifying patients at risk of developing liver cirrhosis one, two, and three years prior to diagnosis. Across all prediction windows, the XGBoost models achieved consistently higher discriminative performance, with AUC improvements of approximately 0.10–0.12 compared with FIB-4. These findings highlight the limitations of traditional rule-based indices and underscore the potential of machine learning approaches to improve early risk stratification for cirrhosis in patients with fatty liver disease.

The superior performance of the machine learning models is not unexpected given the fundamental differences in model design. FIB-4 relies on a small number of laboratory values combined through a fixed linear formula, implicitly assuming constant and independent contributions of each variable across all patients. While this simplicity enables ease of use, it constrains predictive accuracy and limits adaptability across heterogeneous populations. In contrast, the XGBoost models integrate a wide range of demographic characteristics, comorbid conditions, laboratory measures, and vital signs, capturing nonlinear relationships and higher-order interactions that more closely reflect the complex, multifactorial pathophysiology of cirrhosis progression. This ability to leverage longitudinal EHR data and model subtle patterns likely explains the improved discrimination observed, particularly in earlier prediction windows where clinical signals may be less pronounced.

Importantly, the advantage of machine learning was maintained even as the prediction horizon extended to three years before diagnosis, a clinically meaningful timeframe for preventive intervention. Although predictive performance declined with longer horizons for both approaches, the relative gap between the machine learning models and FIB-4 persisted. This suggests that ML-based models are better suited to detecting early risk trajectories rather than relying on late-stage

laboratory abnormalities that are more directly captured by conventional fibrosis scores. From a clinical perspective, this capability is critical, as earlier identification enables timely lifestyle modification, treatment of underlying metabolic risk factors, closer monitoring, and appropriate referral to hepatology before irreversible liver damage occurs.

Beyond predictive accuracy, a key strength of the proposed approach lies in its compatibility with routine clinical workflows. Unlike imaging-based modalities such as transient elastography, the machine learning models rely exclusively on structured EHR data that are already collected during standard care. Once trained and validated, these models can be deployed as automated background processes within the EHR, continuously updating risk estimates as new data become available. This contrasts with FIB-4, which requires manual calculation or explicit clinician initiation and is typically applied at a single point in time rather than longitudinally.

Integration of machine learning predictions into care workflows also enables more actionable clinical decision support. Rather than providing a binary rule-out or rule-in classification, ML models can generate individualized risk probabilities that support tiered care pathways. For example, low-risk patients could continue routine monitoring in primary care, intermediate-risk patients could receive targeted laboratory follow-up or lifestyle counseling, and high-risk patients could be flagged automatically for hepatology referral or advanced testing. Such stratification aligns well with population health and value-based care models, where efficient allocation of specialist resources is essential.

Moreover, the use of EHR-based machine learning supports scalability and equity in cirrhosis screening. Because the required inputs are routinely available across diverse healthcare settings, including community and rural clinics, ML-based risk assessment can extend beyond tertiary centers where advanced imaging is available. This is particularly relevant given the observed associations between rural-urban status and cirrhosis risk in our cohort. Automated ML tools may help mitigate disparities by identifying high-risk patients who might otherwise remain undiagnosed until late-stage disease.

Several limitations should be acknowledged. This study was conducted using data from a single academic health system, which may limit generalizability. External validation across multiple institutions and patient populations will be necessary before widespread implementation. Additionally, although tree-based models such as XGBoost offer strong performance, their complexity can limit interpretability. Future work should explore explainability techniques to enhance clinician trust and facilitate clinical adoption. Finally, prospective studies are needed to evaluate whether integrating ML-based risk prediction into clinical workflows leads to improved patient outcomes compared with existing screening strategies.

## Conclusion

Our study demonstrates that ML models substantially outperform the traditional FIB-4 score in predicting future liver cirrhosis, achieving consistently higher discrimination across 1-, 2-, and 3-year prediction horizons. By leveraging routinely available EHR data and capturing nonlinear interactions among demographics, comorbidities, laboratory results, and vital signs, the ML approach provides more accurate and earlier risk stratification than fixed, rule-based indices.

Importantly, these models can be integrated directly into clinical workflows as automated decision-support tools, enabling proactive identification of high-risk patients, timely referral, and targeted intervention. Such integration has the potential to move cirrhosis care from reactive diagnosis toward earlier, population-scale prevention and management.

## References

1. Gan C, Yuan Y, Shen H, et al. Liver diseases: epidemiology, causes, trends and predictions. *Signal Transduct Target Ther.* 2025;10(1):33. doi:10.1038/s41392-024-02072-z
2. Vaz J, Strömberg U, Midlöv P, Eriksson B, Buchebner D, Hagström H. Unrecognized liver cirrhosis is common and associated with worse survival in hepatocellular carcinoma: A nationwide cohort study of 3473 patients. *J Intern Med.* 2023;293(2):184-199. doi:10.1111/joim.13570
3. Flamm SL. Key Insights and Clinical Pearls in the Identification and Management of Cirrhosis and Its Complications. *Am J Med.* 2024;137(10):929-938. doi:10.1016/j.amjmed.2024.05.015
4. Lee S, Saffo S. Evolution of care in cirrhosis: Preventing hepatic decompensation through pharmacotherapy. *World J Gastroenterol.* 2023;29(1):61-74. doi:10.3748/wjg.v29.i1.61
5. Villanueva C, Tripathi D, Bosch J. Preventing the progression of cirrhosis to decompensation and death. *Nat Rev Gastroenterol Hepatol.* 2025;22(4):265-280. doi:10.1038/s41575-024-01031-x
6. Neuberger J, Cain O. The Need for Alternatives to Liver Biopsies: Non-Invasive Analytics and Diagnostics. *Hepatic Med Evid Res.* 2021;13:59-69. doi:10.2147/HMER.S278076
7. Sumida Y, Nakajima A, Itoh Y. Limitations of liver biopsy and non-invasive diagnostic tests for the diagnosis of nonalcoholic fatty liver disease/nonalcoholic steatohepatitis. *World J Gastroenterol.* 2014;20(2):475-485. doi:10.3748/wjg.v20.i2.475
8. Tsoneva DK, Ivanov MN, Vinciguerra M. Liquid Liver Biopsy for Disease Diagnosis and Prognosis. *J Clin Transl Hepatol.* 2023;11(7):1520-1541. doi:10.14218/JCTH.2023.00040
9. Castéra L, Vergniol J, Foucher J, et al. Prospective comparison of transient elastography, Fibrotest, APRI, and liver biopsy for the assessment of fibrosis in chronic hepatitis C. *Gastroenterology.* 2005;128(2):343-350. doi:10.1053/j.gastro.2004.11.018
10. Kumari B, Kumar R, Sharma S, et al. Diagnostic Accuracy of FIB-4 and FIB-5 Scores as Compared to Fibroscan for Assessment of Liver Fibrosis in Patients With Non-Alcoholic Fatty Liver Disease. *Cureus.* Published online August 31, 2021. doi:10.7759/cureus.17622
11. Metwally K, Elsabaawy M, Abdel-Samiee M, Morad W, Ehsan N, Abdelsamea E. FIB-5 versus FIB-4 index for assessment of hepatic fibrosis in chronic hepatitis B affected patients. *Clin Exp Hepatol.* 2020;6(4):335-338. doi:10.5114/ceh.2020.102157

12. Ng K, Steinhubl SR, deFilippi C, Dey S, Stewart WF. Early Detection of Heart Failure Using Electronic Health Records. *Circ Cardiovasc Qual Outcomes*. Published online November 2016. Accessed September 25, 2018.  
<https://www.ahajournals.org/doi/abs/10.1161/CIRCOUTCOMES.116.002797>
13. Wang R, Miao Z, Liu T, et al. Derivation and Validation of Essential Predictors and Risk Index for Early Detection of Diabetic Retinopathy Using Electronic Health Records. *J Clin Med*. 2021;10(7):1473. doi:10.3390/jcm10071473
14. Kansal A, Gao M, Balu S, et al. Impact of diagnosis code grouping method on clinical prediction model performance: A multi-site retrospective observational study. *Int J Med Inf*. 2021;151:104466. doi:10.1016/j.ijmedinf.2021.104466
15. Malecki SL, Loffler A, Tamming D, et al. Development and external validation of tools for categorizing diagnosis codes in international hospital data. *Int J Med Inf*. 2024;189:105508. doi:10.1016/j.ijmedinf.2024.105508
16. Rural-Urban Continuum Codes | Economic Research Service. Accessed December 18, 2025.  
<https://www.ers.usda.gov/data-products/rural-urban-continuum-codes>
17. Quan H, Sundararajan V, Halfon P, et al. Coding Algorithms for Defining Comorbidities in ICD-9-CM and ICD-10 Administrative Data. *Med Care*. 2005;43(11):1130. doi:10.1097/01.mlr.0000182534.19832.83
18. Chen T, Guestrin C. XGBoost: A Scalable Tree Boosting System. In: *Proceedings of the 22nd ACM SIGKDD International Conference on Knowledge Discovery and Data Mining*. KDD '16. Association for Computing Machinery; 2016:785-794. doi:10.1145/2939672.2939785
19. Kumar D, Sood SK, Rawat KS. Early health prediction framework using XGBoost ensemble algorithm in intelligent environment. *Artif Intell Rev*. 2023;56(1):1591-1615. doi:10.1007/s10462-023-10565-6
20. Vallet-Pichard A, Mallet V, Nalpas B, et al. FIB-4: An inexpensive and accurate marker of fibrosis in HCV infection. comparison with liver biopsy and fibrotest. *Hepatology*. 2007;46(1):32-36. doi:10.1002/hep.21669

## Appendix

Table A1. Cohort characteristics for the 2-year prediction

	Overall	Controls	Cases	p-value
Patient Counts	1981	1473	508	
Gender				<0.001
Female	1132	885	247	
Male	848	587	261	
Unknown	1	1	0	
Race				0.051
Native American	4	3	1	
Asian	58	49	9	
Black	683	524	159	
Decline	7	7	0	
Hispanic	22	18	4	
White	1207	872	335	
Marital Status				0.265
Divorced	229	167	62	
Life Partner	10	8	2	
Married	945	715	230	
Separated	26	22	4	
Single	563	399	164	
Unknown	35	27	8	
Widowed	173	135	38	
Rural-Urban Status				<0.001
Metro, ≥1 million	1542	1186	356	
Metro, 250,000 to 1 million	114	73	41	
Metro, <250,000	104	64	40	
Nonmetro, ≥20,000, adjacent to metro	112	76	36	
Nonmetro, ≥20,000, not adjacent to metro	10	6	4	
Nonmetro, 5,000 to 20,000, adjacent to metro	37	25	12	
Nonmetro, 5,000 to 20,000, not adjacent to metro	6	2	4	
Nonmetro, <5,000, adjacent to metro	31	23	8	
Nonmetro, <5,000, not adjacent to metro	25	18	7	
Age, mean (SD)	55.3 (13.5)	55.2 (13.8)	55.3 (12.7)	0.900
Vitals/Labs, mean (SD)				
CCI	0.3 (0.4)	0.3 (0.4)	0.3 (0.3)	0.634
BMI	33.2 (8.1)	33.6 (8.1)	32.2 (7.9)	<0.001
DBP	79.4 (6.9)	79.2 (6.8)	80.0 (6.9)	0.025
SBP	132.0 (12.3)	131.7 (12.3)	132.9 (12.3)	0.065
ALT (LOINC: 1742-6)	36.0 (41.3)	32.6 (38.8)	46.1 (46.3)	<0.001
Albumin (LOINC: 1751-7)	4.3 (7.8)	4.5 (9.0)	3.9 (0.4)	0.019
AST (LOINC: 1920-8)	35.1 (34.5)	30.4 (29.3)	48.7 (43.8)	<0.001
Bilirubin (LOINC: 1975-2)	0.7 (0.6)	0.6 (0.5)	0.9 (0.8)	<0.001
Platelets (LOINC: 26515-7)	234.1 (79.6)	241.8 (75.7)	211.8 (86.2)	<0.001
Protein (LOINC: 2885-2)	7.1 (0.6)	7.0 (0.5)	7.1 (0.6)	0.003
PT (LOINC: 5902-2)	14.2 (2.6)	14.1 (2.5)	14.5 (2.9)	0.002
ALP (LOINC: 6768-6)	89.3 (57.8)	83.7 (40.0)	105.7 (89.6)	<0.001
Hemoglobin (LOINC: 718-7)	13.0 (1.7)	13.0 (1.7)	13.0 (1.8)	0.597

Table A2. Cohort characteristics for the 3-year prediction

	Overall	Controls	Cases	p-value
Patient Counts	1470	1099	371	
Gender				<0.001
Female	849	665	184	
Male	621	434	187	
Race				0.019
Native American	3	2	1	
Asian	43	36	7	
Black	486	381	105	
Decline	6	6	0	
Hispanic	14	13	1	
White	918	661	257	
Marital Status				0.709
Divorced	159	122	37	
Life Partner	8	7	1	
Married	715	537	178	
Separated	19	16	3	
Single	421	305	116	
Unknown	23	16	7	
Widowed	125	96	29	
Rural-Urban Status				0.001
Metro, ≥1 million	1152	892	260	
Metro, 250,000 to 1 million	84	54	30	
Metro, <250,000	68	42	26	
Nonmetro, ≥20,000, adjacent to metro	85	56	29	
Nonmetro, ≥20,000, not adjacent to metro	5	4	1	
Nonmetro, 5,000 to 20,000, adjacent to metro	29	20	9	
Nonmetro, 5,000 to 20,000, not adjacent to metro	6	2	4	
Nonmetro, <5,000, adjacent to metro	22	16	6	
Nonmetro, <5,000, not adjacent to metro	19	13	6	
Age, mean (SD)	54.6 (13.4)	54.6 (13.7)	54.7 (12.6)	0.948
Vitals/Labs, mean (SD)				
CCI	0.3 (0.4)	0.3 (0.4)	0.3 (0.3)	0.936
BMI	33.2 (8.0)	33.3 (7.9)	32.8 (8.2)	0.364
DBP	79.3 (7.0)	79.0 (7.1)	80.1 (6.9)	0.013
SBP	131.6 (12.4)	131.2 (12.2)	132.8 (12.9)	0.039
ALT (LOINC: 1742-6)	35.1 (33.9)	31.9 (30.8)	44.5 (40.2)	<0.001
Albumin (LOINC: 1751-7)	4.4 (8.6)	4.5 (9.9)	3.9 (0.4)	0.052
AST (LOINC: 1920-8)	33.5 (29.0)	29.6 (23.8)	44.9 (38.6)	<0.001
Bilirubin (LOINC: 1975-2)	0.7 (0.6)	0.6 (0.5)	0.8 (0.6)	<0.001
Platelets (LOINC: 26515-7)	235.7 (79.0)	242.6 (77.4)	215.2 (80.3)	<0.001
Protein (LOINC: 2885-2)	7.0 (0.6)	7.0 (0.6)	7.1 (0.6)	<0.001
PT (LOINC: 5902-2)	14.2 (2.7)	14.1 (2.5)	14.6 (3.1)	0.008
ALP (LOINC: 6768-6)	87.7 (55.8)	83.1 (41.3)	101.5 (83.9)	<0.001
Hemoglobin (LOINC: 718-7)	13.1 (1.8)	13.0 (1.8)	13.2 (1.8)	0.078